ELSEVIER

Polymer 41 (2000) 7827–7841

polymer

Tensile stress–strain behaviour of rubberlike networks up to break. Theory and experimental comparison

B. Meissner*

Institute of Macromolecular Chemistry, Academy of Sciences of the Czech Republic, Heyrovsky Sq. 2, 162 06 Prague 6, Czech Republic

Received 22 January 1999; received in revised form 4 June 1999; accepted 3 February 2000

Abstract

A satisfactory description of the tensile stress–strain dependences (SSDs) of lightly crosslinked single-phase networks is not obtained with use of the existing theories (Langevin, van der Waals, slip-link). A combination of the Langevin theory-based James–Guth equation with the phenomenological C_2 term of the Mooney–Rivlin equation (JGC2 equation) is shown to represent the SSDs of a number of networks (bimodal polysiloxane, pre-strained SBR) very well. Hysteresis-based deviations of some networks from the JGC2 equation in the high elongation region can be quantitatively taken into account as an increase in the finite extensibility parameter with extension ratio. The accuracy of the SSD description up to break is generally better than 3–4%.

Keywords: Tensile stress–strain dependence; Rubberlike networks; Theory of rubbber elasticity

1. Introduction

Rubberlike behaviour is typified by a low initial modulus (10^{-1}–10^{1} MPa) and a high tensile strain at break ϵ_b (commonly several hundred percent) with the strain being to a large extent reversible. The tensile strain $\epsilon = (L - L_o)/L_o$ is the relative change of length. It is often expressed in per cent of the original undeformed length L_o and called elongation or extension. The tensile stress–strain dependence (SSD) of most rubberlike networks has a sigmoidal shape. The inflection point of the SSD, ϵ_{infl}, is usually located in the region between 100 and 300% elongation. In the following text, tensile strain (elongation) will be denoted roughly as low, medium and high, with the medium elongation region being defined as that situated in the vicinity of the inflection point ϵ_{infl}, within the limits of, say, 0.85 ϵ_{infl} and 1.15 ϵ_{infl}. In practice, the tensile stress–strain measurements are usually done under non-equilibrium conditions. They belong to fundamental and most frequently used tests, the data obtained giving basic, important and manifold information which is being exploited for quality control, material specification and developmental work. Measurements trying to approach elastic equilibrium are done less frequently, usually when testing molecular and phenomenological theories.

In the past six decades, hundreds of theoretical studies have been devoted to the low-elongation behaviour of rubberlike networks and to experimental testing of theoretical predictions [1,2]. The high-elongation behaviour has received less theoretical attention. In principle, three main approaches are available: the James and Guth theory [3], based on the Langevin chain statistics, the Kilian van der Waals theory [4] and the Edwards–Vilgis theory [5] based on a slip-link model.

In the present paper, the tensile stress–strain dependences obtained on homogeneous (unfilled) rubberlike networks and measured under quasi-equilibrium conditions are analysed in light of the above mentioned theories of rubber elasticity in an effort to develop a general basis for a mathematical description of the SSD in the whole strain range up to break. The description is intended to afford structural interpretation, to be applicable to data without the necessity of preliminary knowledge of material composition or structure, to be simple and to give a good fit to data.

2. Theoretical

2.1. Low-elongation region

Gaussian theory. The equilibrium stress–strain dependence of elastomeric networks in the region of low elongation was qualitatively explained on the basis of the classical Gaussian rubber elasticity theory as early as 1936 [6] and developed further in a number of papers cf. [1,2]. The only

* Tel.: + 420-2-20403384; fax: + 420-2-367981.
E-mail address: meissner@imc.cas.cz (B. Meissner).

0032-3861/00/$ - see front matter
PII: S0032-3861(00)00114-2

parameter of the theory is the shear modulus G which—due to the incompressibility of the network—determines the initial slope of the SED: $(d\sigma/d\epsilon)_{\epsilon=0} = 3\,G$; σ is the nominal stress, i.e. force per unit of undeformed area of cross-section. The Gaussian result for the stress in simple extension is given by

$$\sigma = G\,D \tag{1}$$

$$D = \lambda - 1/\lambda^2 \tag{2}$$

λ is the extension ratio: $\lambda = L/L_o = \epsilon + 1$.

The shear modulus G of the Gaussian network is predicted to be proportional to the concentration ξ (mol/m^3) of independent circuituous paths in the network, called the cycle rank

$$G = \xi \mathrm{R}T \qquad \text{phantom theory [7, 8, 2]} \tag{3}$$

$$G = \frac{\phi}{\phi - 2}\,\xi \mathrm{R}T \qquad \text{affine theory [9, 10, 2]} \tag{4}$$

ϕ is the junction functionality, R the gas constant, and T the absolute temperature. In a perfect network with a concentration of C junctions, the cycle rank $\xi = C(\phi - 2)/2$ and the concentration of network chains, $\nu = C\phi/2$. The modulus of a perfect phantom network devoid of imperfections of any kind (dangling chains, intramolecular loops, entanglements) and containing C (mol/m^3) tetrafunctional junctions is $G = C\mathrm{R}T = (\nu/2)\mathrm{R}T$; that of an affine network is equal to $G = 2C\mathrm{R}T = \nu\mathrm{R}T$. For an imperfect network, Flory [11] defined the term "effective" chains to be those that effectively contribute to the elasticity of the network and related their number ν_{eff} to the cycle rank by $\nu_{\mathrm{eff}} = 2\xi$.

Deviations from the Gaussian equations (1) and (2) at low elongations. A general definition of the so-called reduced stress σ_{red} is given by the relation

$$\sigma_{\mathrm{red}} = \sigma/D \tag{5}$$

In the simple Gaussian theory the reduced stress is independent of the extension ratio. This is not supported by experiment: at low elongations virtually all unswollen rubberlike networks show a decrease in reduced stress with increasing extension ratio.

Phenomenological theory. A simple satisfactory description of the low-elongation behaviour of most single-phase networks is offered by the phenomenological two-parameter equation of Mooney and Rivlin [12,13]. Its first term (the C_1 term) has the same λ-dependence as the result of the Gaussian theory (Eq. (2)), the second term (the C_2 term) introduces the necessary decrease in reduced stress with increasing extension ratio

$$\sigma_{\mathrm{MR}} = 2C_1 D + 2C_2(1 - 1/\lambda^3) \tag{6}$$

$$\sigma_{\mathrm{MR}}/D = 2C_1 + 2C_2/\lambda \tag{7}$$

Relations between the experimentally determined Mooney–Rivlin parameters, C_1, C_2, and the structural parameters of the networks were studied in a number of papers, cf. [2,14–17]. As a rule, the measured modulus is higher than that calculated from the knowledge of the network structure and using the Gaussian equations (1)–(4). The latter effect has often been ascribed to the presence of chain entanglements trapped between chemical crosslinks [15].

Molecular theories. In the phantom theory [2,7,8], the network junctions are assumed to be freely fluctuating in space. In the affine theory [2,9,10] they are assumed to move affinely with macroscopic deformation, which assumption suppresses the fluctuations of the chain ends. Both these theories predict a strain-independent reduced stress σ_{red} (zero C_2) but different values of the modulus since junction fluctuations lead to a decrease in the modulus. The presence of chain entanglements is argued to lead to a deformation-dependent contribution to the modulus. The constrained-junction model [18,19] and slip-link model [20] (see below) are both based on the postulate that, upon stretching, the space available to a chain along the direction of the stretch is increased. This results in an increase in the freedom of the chain to fluctuate and in a decrease of the reduced modulus, in qualitative agreement with the Mooney–Rivlin equation.

2.2. Medium- and high-elongation region

Non-Gaussian theory based on Langevin chain statistics. In the region of high elongation, the experimental stress of rubberlike networks increases much more steeply than predicted by the Gaussian theory. The first explanation for this type of behaviour was based on the argument of finite extensibility of polymer chains which is reached at high extensions [3]. The latter effect was taken into account by replacing the Gaussian chain statistics with non-Gaussian statistics and by using a suitable model for the network of non-Gaussian chains. The results based on Langevin chain statistics and on the three-chain [3] and eight-chain [21] network models, respectively, are mentioned here.

The three-chain network model used by James and Guth [3] leads to the following relationship for nominal stress, σ_3 (see also Treloar [1])

$$\sigma_3 = G_3(\lambda_{\mathrm{m}}/3)\{\mathscr{L}^{-1}(\lambda/\lambda_{\mathrm{m}}) - (1/\lambda^{3/2})\mathscr{L}^{-1}(1/\lambda^{1/2}\lambda_{\mathrm{m}})\}. \tag{8}$$

$\mathscr{L}$ is the Langevin function ($\mathscr{L}(x) = \coth(x) - 1/x$) and $\mathscr{L}^{-1}$ is the inverse Langevin function.

The James and Guth (JG) equation contains two parameters: the shear modulus, G_3, which determines the initial slope of the SSD, and the limiting (highest possible) extension ratio, λ_{m}, where the stress tends to infinity. G_3 is proportional to the *number* of network chains per unit volume while λ_{m} of a phantom network is determined by the *length* of network chains and is equal to the square root of the number Z_{c3} of statistical segments in the network chain:

$$\lambda_{\mathrm{m}} = Z_{\mathrm{c3}}^{1/2} \tag{9}$$

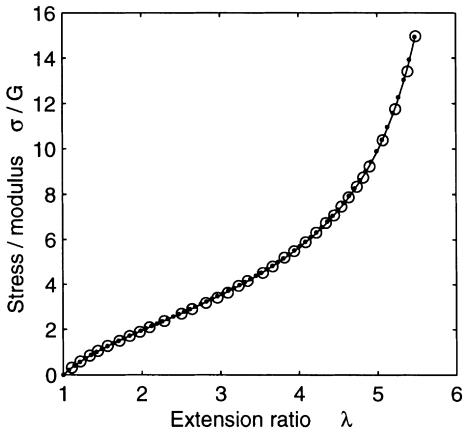

Fig. 1. Comparison of the stress–strain curves calculated using the four-chain (tetrahedral) model with non-affine displacement of the mean position of the central junction point [1] with the predictions of the three-chain [3] and eight-chain [21] models, respectively. Open circles: four-chain model, $Z_{c,4} = 25$ (Ref. [1, p. 119]). Full curve: three-chain model, $G_3 = 1.04$, G_4, $Z_{c,3} = 41.6$, $\lambda_{m,3} = Z_{c,3}^{1/2} = 6.45$. Full circles: eight-chain model, $G_8 = 0.99$ G_3, $Z_{c,8} = 14$, $\lambda_{m,8} = 6.45$.

In the region of low elongation and not too small Z_{c3}, Eq. (8) reduces to the Gaussian result given by Eqs. (1) and (2). Eq. (8) predicts a constant reduced stress at low elongations and a gradual increase in reduced stress starting from the inflection point region. In a perfect tetrafunctional phantom network, the parameters G_3, λ_m, are related in a simple manner: $Z_{c3} = M_c/M_s$, $M_c = \rho/2C$ and, consequently:

$$\lambda_m = G_3^{-1/2}(\rho RT/2M_s)^{1/2}.$$

M_c is the molar mass of chain per crosslinked unit and is a measure of molar mass of a network chain between neighbouring junction points, M_s is the molar mass of a statistical segment, ρ is the density. Thus, according to the James–Guth theory an increase in modulus, brought about by an increase in junction point concentration resulting in a shortening of network chains, should be accompanied by a loss of extensibility. For real imperfect networks, this prediction is correct, at least qualitatively. It manifests itself, e.g. in a decrease in elongation at break with increasing modulus in a series of networks differing in junction point concentration.

The eight-chain network model used by Arruda and Boyce [21] leads to the nominal stress σ_8 in the form

$$\sigma_8 = G_8(Z_{c8}^{1/2}/3)(D/\lambda_s)\mathscr{L}^{-1}(\lambda_s/Z_{c8}^{1/2}) \quad (10)$$

where

$$\lambda_s = [(\lambda^2 + 2/\lambda)/3]^{1/2} \quad (11)$$

Z_{c8} is the number of statistical segments in the network chain of the eight-chain model. In the region of low elongation and not too small Z_{c8}, Eq. (10) reduces to the Gaussian result. The limiting extension ratio λ_m follows from Eq. (10). The stress singularity $\sigma_8 \to \infty$ is reached when $\lambda_s/Z_{c8}^{1/2} = 1$ and, inserting for λ_s from Eq. (11), we get

$$\lambda_m^2 + 2/\lambda_m = 3Z_{c8} \quad (12)$$

Arruda and Boyce claim that their eight-chain model has the advantage over the three-chain model in giving a better prediction for the stress in biaxial extension. In the present study, however, we limit ourselves to uniaxial extension. Under the condition $Z_{c8} = Z_{c3}$, the limiting extension ratio λ_m of the eight-chain model calculated from Eq. (12) is higher than that of the three-chain model (Eq. (9)) by a factor of approx. $3^{1/2}$. Consequently, at a given high elongation, the stress σ_8 is lower than σ_3. However, for our purpose—description of an experimental SSD by a suitable function—it is the limiting extension ratio which is of primary importance. Therefore, we will compare the two models under the condition of equal limiting extension ratio, i.e. when Z_{c8}, Z_{c3} are related through Eqs. (12) and (9):

$$Z_{c8} = (Z_{c3} + 2/Z_{c3}^{1/2})/3 \quad (13)$$

In Fig. 1, the points denoted by open circles were taken from the SSD calculated by Treloar [1] for the four-chain tetrahedral model (non-affine displacement of the mean position of the central junction point; number of statistical segments in the network chain $Z_{c4} = 25$). The full curve is a three-chain model best fit to the four-chain (non-affine) model result. The curve is drawn using Eq. (8) and parameter values $G_3 = 1.04$, G_4, $Z_{c3} = 41.6$. Full circles were calculated using the eight-chain model Eq. (10), modulus value $G_8 = 0.99$ G_3 and the number $Z_{c8} = 14$ of statistical segments in the network chain calculated from $Z_{c3} = 41.6$ using Eq. (13). It can be seen that with a suitable choice of parameter values, the three non-Gaussian network models predict essentially the same stress–strain dependence. For shorter network chains (smaller M_c), the differences between predictions of the three-chain model and the eight-chain model increase but remain insignificant. It may be concluded that as regards its shape, a given SSD can be described by equations based on the three different non-Gaussian network models with a similar degree of accuracy. On the other hand, different values of Z_c and, consequently, of the molar mass of the statistical segment, M_s, will be obtained. From the results shown in Fig. 1, it follows that the values of the molar mass of statistical segment M_{s3}, M_{s4} and M_{s8} calculated for a network with a given M_c (and λ_m) using the three-chain, four-chain (non-affine) and eight-chain models, respectively, have different values. The latter are in an approximate ratio $M_{s3} : M_{s4} : M_{s8} = 3 : 5 : 9$. This result suggests that the physical significance of the M_s values obtained in this way should not be overestimated.

The Morris equation [22] is a three-parameter combination of a Langevin-type theory (the stress being given in the form of a power series expansion) and of the C_2 term of the

Mooney–Rivlin equation

$$\sigma = 2C_1D\left\{1 + \frac{3}{25Z_c}\left(3\lambda^2 + \frac{4}{\lambda}\right) + \frac{297}{6125Z_c^2}\left(5\lambda^2 + 8\lambda + \frac{8}{\lambda}\right) + \frac{12312}{2205000Z_c^2}\left(35\lambda^6 + 60\lambda^3 + 72 + \frac{64}{\lambda^3}\right)\cdots\right\} + 2C_2\left(1 - \frac{1}{\lambda^3}\right) \quad (14)$$

(subscript 3 in Z_{c3} has been dropped here). The applicability of Eq. (14) is limited to the low- and medium-elongation region only and a satisfactory description of the SSD of natural rubber networks at low and medium elongations up to slightly above the inflection point was obtained by Morris [22]. Recently Klüppel [23,24] has applied the Morris approach to his NR and SBR networks and found a good data description up to slightly above the minimum of reduced stress. At higher λ, the experimental stress increased at a much lower rate than the stress calculated from Eq. (14). Klüppel ascribed this effect to the rupture of single chains by increasing stress. However, such an explanation should be accepted with caution. Simple swelling tests on samples taken from unextended and extended (or even ruptured) dumbbell specimens do not indicate any significant change in the network density with increasing elongation.

The van der Waals theory of elasticity. Both finite chain extensibility and intermolecular interactions are taken into account in this theory that derives the following three-parameter equation (Kilian [4]):

$$\sigma = \mathrm{GD}\left[\frac{1}{1 - D/D_m} - aD\right] \quad (15)$$

In a later paper [25], the equation is given in a modified form:

$$\sigma = \mathrm{GD}\left[\frac{1}{1 - A} - aB\right]$$

$$A = (\phi/\phi_m)^{1/2};\ B = \phi^{1/2};\ \phi = \tfrac{1}{2}(\lambda^2 + 2/\lambda - 3); \quad (16)$$

$$\phi_m = \tfrac{1}{2}(\lambda_m^2 + 2/\lambda_m - 3)$$

D_m is the value of D at the maximum extension ratio λ_m, a is a phenomenological parameter called the 'global interaction parameter'. Relationships of G and λ_m to the network structure are given by the expressions $G = \rho RT/M_c$ (affine network), $\lambda_m = (M_c/M_s)^{1/2}$. No prediction as to the value of a is offered by the theory.

The slip-link model [5,20]. This model considers a randomly crosslinked polymer melt where some trapped entanglements between crosslinks (between four-functional network junctions) are present. At low deformations the trapped entanglements are able to slide and behave as slip-links. This leads to a decrease in the reduced stress, as derived by Ball et al. [20]. Making use of his result, Edwards and Vilgis have shown [5] that at high deformations, the trapped entanglements restrict the extensibility and give rise to a strong increase in the elastic stress. From their equation for free energy [5], the expression for stress in simple extension has been calculated here in the following form (equations for σ_s given in the authors' papers [5,26,27] seem to contain printing errors)

$$\sigma = \sigma_c + \sigma_s \qquad \sigma_c = N_c kTD\left(\frac{1 - \alpha^2}{A^2} - \frac{\alpha^2}{A}\right)$$

$$\sigma_s = N_s kTD\left\{\frac{(1 - \alpha^2)(1 + \eta)}{A^2}\left[\frac{(1 - \eta^2\lambda)\lambda^2 A}{B^2(\lambda + \eta)^2} + \alpha^2\left(\frac{\lambda^2}{B} + \frac{2}{\lambda + \eta}\right)\right] + \frac{\eta\lambda}{B(\lambda + \eta)} - \frac{\alpha^2}{A}\right\}$$

$$A = 1 - \alpha^2(\lambda^2 + 2/\lambda);\ B = 1 + \eta\lambda^2;\ \lambda_m = 1/\alpha \quad (17)$$

The Edwards–Vilgis Eq. (17) contains four parameters. N_c ($1/m^3$) is the concentration of crosslinks, N_s ($1/m^3$) is the concentration of slip-links, λ_m is a measure of network extensibility (maximum attainable extension ratio), η is a dimensionless slip parameter. In the absence of slip-links ($N_s = 0$) the modulus is given by $G = N_c kT$ which is the result for a perfect tetrafunctional phantom network ($G = CRT$). In the Ball et al. theory [20] the slip parameter is a function of the relative amount of slip x and is calculated as

$$\eta(x) = x^{-2}(x - x^2 + (2/3)x^3 - (1/2)(1 - e^{-2x})) \quad (18)$$

The relative amount of slip is expressed as the length of slip a divided by $L_{cs} = L/(2N_c + 2N_s)$ where L is the total contour length of all chains present [20] (in the present paper L is expressed per unit of volume, m/m^3). The expression given by Ball et al. for L_{cs} is the length of chain per linked (i.e. both crosslinked and entangled) structural unit and is a measure of the chain length between network junctions (both crosslinks and slip-links). Ball et al. assume that each slip-link can on average slide as far as the centres of its topologically neighbouring links. In such case, the relative amount of slip a/L_{cs} is unity and the function $\eta(x)$ attains its theoretically highest value $\eta(1) = 0.2343$. It should be noted that the result of Ball et al. is included in the Edwards–Vilgis expression for free energy and that for $\alpha = 0$, Eq. (17) yields the Ball equation for stress as its special case. Therefore, the definition of η and conclusion about its theoretical value should remain valid even for Eq. (17). Edwards and Vilgis, however, give the following statement in conclusion of their paper: 'In the theoretical model given by the replica calculation, η is a fixed value but this cannot be true for real situation in a network. Since η is a measurement for the slip, it can be related to the length between two

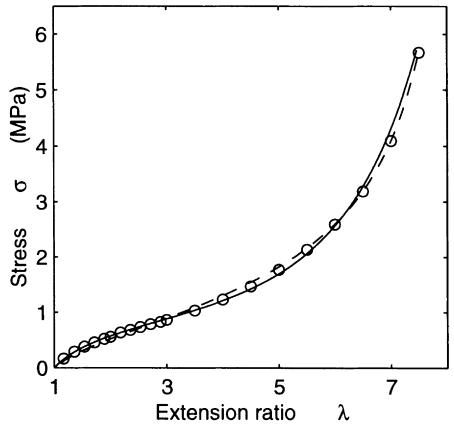

Fig. 2. Comparison of the Treloar data on a NR network [1] (points) with theoretical equations (curves). Linear co-ordinates. Dashed curve: Eq. (8), $G = 0.286$ MPa, $\lambda_m = 8.8$. Full curve: Eq. (16), $G = 0.372$, $\lambda_m = 10.29$, $a = 0.285$.

crosslinks since this is the maximum value of slip.' From this one could infer that the highest possible slip length is not L_{cs} but L_c and the highest possible relative slip should then be $L_c/L_{cs} = (N_c + N_s)/N_c$. This quantity is much higher than unity at low degrees of crosslinking and with increasing N_c, it decreases in the limit to unity. In a later paper [26], Vilgis redefines the slip parameter as a ratio of the entanglement distance a_E and the contour length of chains between crosslinks ($\eta_V = a_E/L_c$) and arrives at the conclusion that η_V is independent of the degree of crosslinking. However, if one starts from the Vilgis definition, one should expect η_V to be much smaller than unity at low degrees of crosslinking (i.e. if L_c is much larger than the entanglement distance) and larger than unity at high degrees of crosslinking (i.e. if L_c becomes smaller than the entanglement distance). To escape from this somewhat unclear situation, the original, theoretically well founded concept of Ball et al. should be preferred.

The Edwards–Vilgis theory relates the λ_m parameter to the distance a_E between entanglements:

$$\lambda_m = a_E/l_s \tag{19}$$

l_s is the length of a statistical segment. According to Eq. (19), the network extensibility should be determined by the length of chains between entanglements. The latter may be expected to be independent of the presence and amount of chemical crosslinks and thus the prediction following from Eq. (19) stands in a sharp contrast to the Langevin result given by Eq. (9).

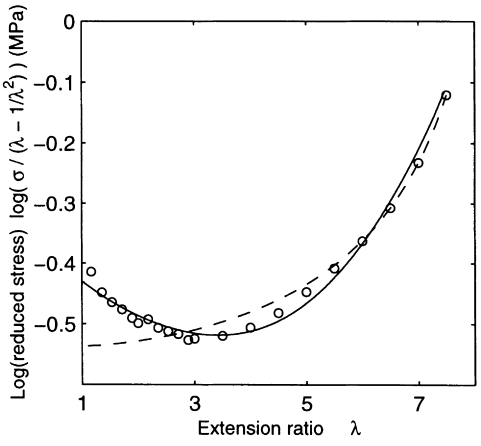

Fig. 3. Comparison of the Treloar data on a NR network [1] (points) with theoretical equations (curves). Co-ordinates: log(reduced stress) vs. extension ratio (see Fig. 2).

3. Comparison of theoretical equations with experiment

3.1. James and Guth

A measure of agreement of the Arruda–Boyce equation with Treloar's data on a natural rubber (NR) network [1] in simple extension has recently been characterised by Arruda and Boyce [21] as satisfactory. A similar conclusion should apply to the James–Guth equation. An experiment–theory comparison is illustrated in Fig. 2 where the data are plotted in linear co-ordinates. The deviation of the data from the fitted curve does not seem to be large. However, relative deviation is better visible in a logarithmic plot or, even more clearly, if the logarithm of reduced stress is plotted vs. the extension ratio. In Fig. 3, such type of plot shows systematic negative deviations of some 5% in the medium elongation region and systematic positive deviations exceeding 25% in the low elongation region. Such result is not satisfactory and disqualifies the two-parameter Eqs. (8) and (10) for use in the SSD representation.

3.2. Kilian

A satisfactory description of experimental stress–strain curves by the van der Waals Eq. (15) was demonstrated for a number of networks of medium network density [28] and is also seen in Figs. 2 and 3. However, the fit of Eq. (15) to the SSD of lightly crosslinked networks is less satisfactory [28]. To test this feature once more, the experimental data of Ikeda et al. [29,30] obtained on a lightly crosslinked SBR with a high C_2/C_1-ratio (see its Mooney–Rivlin plot in Fig. 4) are compared with Eq. (16) in Fig. 5. The parameter values are adjusted so as to obtain a correct value of the initial slope and a satisfactory fit in the high elongation region. The resulting experiment–theory deviations (curve 3) in the medium elongation region are unacceptably large (more than 40%) and this, together with a somewhat unclear physical meaning of the global interaction parameter, makes the van der Waals Eq. (16) less suitable for the purpose outlined in Section 1. The type of fit of Eq. (15) to the data in Fig. 5 is similar to that of Eq. (16).

3.3. Edwards and Vilgis

The slip-link model predictions were tested by Thirion

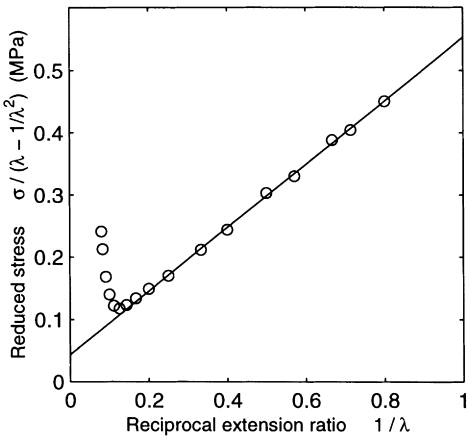

Fig. 4. Comparison of the Ikeda data [29,30] on a lightly crosslinked network (SBR A, points) with Eq. (6) (straight line). Co-ordinates: reduced stress vs. reciprocal extension ratio. Straight line calculated for nine points (least-squares method). $C_1 = 0.0219$ MPa, $C_2 = 0.254$ MPa.

and Weil [31] who compared the Ball equation (i.e. Eq. (17) with $\alpha = 0$) with data on NR and SBR networks in the low-elongation region. To obtain an optimum fit, they had to replace the theoretical value of $\eta = 0.234$ by a higher value of 0.4. Brereton and Klein [32] obtained even higher values of η (up to 1.4) when they compared Eq. (17) with their data on electron-beam-crosslinked PE networks. With increasing dose, the values of N_c and N_s increase as expected while λ_m decreases. For doses 2.4, 3.5, 6.0 M^{rad} the λ_m values were ∞, 25, 14.3, respectively. This finding contradicts the theoretical expectation expressed by Eq. (19). Edwards and Vilgis [5] themselves tested their Eq. (17) and showed a very good fit to experimental data of Mullins [33] when using the theoretical value of $\eta = 0.2$.

Further experimental testing of Eq. (17) is done here. The data of Mullins [33] taken from the original paper are plotted in Fig. 6 in the co-ordinates of logarithm of reduced

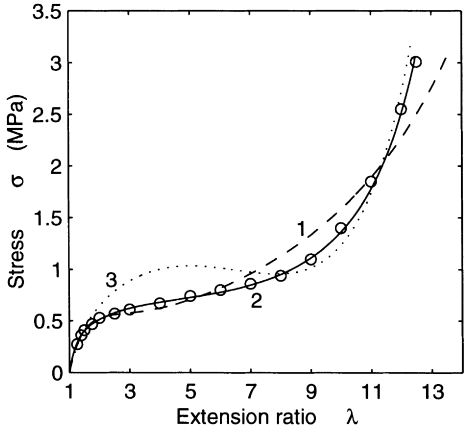

Fig. 5. Comparison of the Ikeda data [29,30] on the network SBR A (points) with theoretical equations. Curve 1—Eq. (17), $\eta = 0.234$, $N_c kT = 0.1$ MPa, $N_s kT = 0.57$ MPa, $\lambda_m = 24$. Curve 2—Eq. (17), $\eta = 2.4$, $N_c kT = 0.015$ MPa, $N_s kT = 6.5$ MPa, $\lambda_m = 16.9$. Curve 3—Eq. (16), $G = 0.45$ MPa, $\lambda_m = 19$, $a = 0.26$.

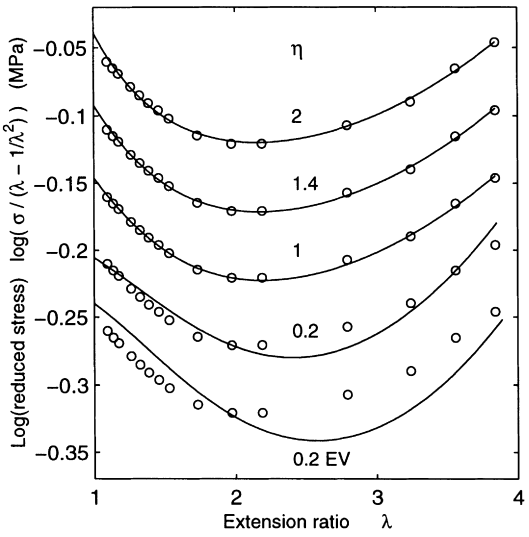

Fig. 6. Comparison of the Mullins data on a NR network [33] (points) with Eq. (17) (curves) using the following parameter values:

η	$N_c kT$ (MPa)	$N_s kT$ (MPa)	λ_m
0.2 EV	0.24	0.42	7.5
0.2	0.27	0.35	7.5
1	0.351	0.715	9.0
1.4	0.342	1.07	9.0
2.0	0.325	1.74	9.0

0.2 EV: parameter values given by Edwards and Vilgis [5]. Points and curves designated 0.2, 1, 1.4, 2.0 are successively shifted upwards by 0.05.

stress vs. extension ratio. (It should be noted that in the Mullins paper, the reduced stress *divided by* two is plotted on the ordinate. This was not taken into account by Edwards and Vilgis and, therefore, the values of N_c and N_s they obtained [5] are to be doubled.) The curves in Fig. 6 are calculated from Eq. (17) for several values of η and the remaining three parameters are adjusted to obtain the best fit to the data. In Fig. 6, the lowest curve ($\eta = 0.2$, EV) is drawn using the parameter values given by Edwards and Vilgis (with N_c, N_s, multiplied by two). The fit to the data is not satisfactory, contrary to the conclusion of Edwards and Vilgis [5]. The other theoretical curves with their experimental points are gradually shifted upwards by 0.05. The curve designated 0.2 is drawn with modified values of N_c and N_s, but the fit remains unsatisfactory. A good data description is obtained with η in the range between 1 and 2. An increase in η is accompanied by a pronounced growth of N_s (for $\alpha = 0$, one gets from Eq. (17): $(d\sigma_s/d\lambda)_{(\lambda=1)} = 3N_s kT/(1 + \eta)^2$; therefore, to satisfy the requirement for a given initial slope, the N_s value must increase with increasing η).

The Edwards–Vilgis equation has been further tested in Fig. 5 using the Ikeda data on SBR [29,30]. The parameter values for curves 1 and 2 are given in Fig. 5. Similarly as previously, a satisfactory data representation can only be obtained with values of the slip parameter which are several times higher than the theoretically derived value and the

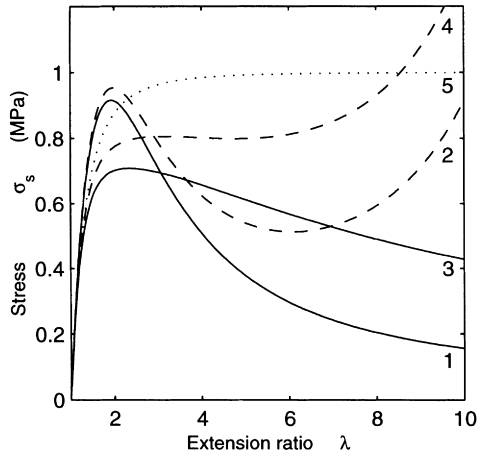

Fig. 7. Dependence of σ_s on λ (Eq. (17)) for different parameter values (curves 1–4, $N_s kT/(1+\eta)^2 = 1$ MPa) compared with the λ-dependence of the C_2 term (curve 5, $2C_2 = 1$ MPa)

Curve	η	α	λ_m
1	0.234	0	∞
2	0.234	0.0625	16
3	1.5	0	∞
4	1.5	0.0625	16

changes of N_s and N_c, accompanying the increase of η lead to rather unrealistic values: N_s becomes very high and N_c drops almost to zero while the λ_m parameter decreases from 24 to 16.9.

The following conclusions may be drawn:

1. If the slip parameter is prescribed to have its theoretical value of 0.234, then Eq. (17) is not able to satisfactorily describe the experimental stress–strain data.
2. Eq. (17) is able to give a satisfactory fit to some experimental stress–strain data only if all four parameters are allowed to be adjustable. The optimum-fit procedure, however, may lead to unrealistic values of N_s, N_c, and yield values of the slip parameter which are too high to be theoretically justified unless one accepts that the length of slip may be several times longer than the length of the chain between network junctions (both crosslinks and slip-links). From Eq. (18), one calculates values of $\eta = 1.4$ and 2.5 for $x = 3.2$ and 5, respectively.
3. For $\alpha = 0$, $\eta = 0.234$, the predicted λ-dependence of σ_s has a sharp maximum (which becomes less pronounced with increasing α); for $\alpha = 0$, $\eta > 1$, the maximum is less sharp (Fig. 7) and the shape of the dependence approaches that of the C_2 term of the Mooney–Rivlin equation which is known to generally give a good data representation. Thus, the shortcomings of Eq. (17) seem to be associated with the fact that its low- and medium-elongation prediction of σ_s based on the theoretical value of the slip parameter does not imitate the Mooney–Rivlin C_2 term closely enough.
4. The network extensibility is predicted to be insensitive to the crosslink concentration. This is not in accord with experience and seems to be the main controversial point of the Edwards–Vilgis theory.
5. Analysis of low-elongation data on the basis of the Ball equation (as done by Thirion and Weil) may not necessarily give the same result as that performed on the basis of Eq. (17) since the finite extensibility contribution to the stress persists and is appreciable down to low elongations (see Fig. 7). It is interesting to note that the finite extensibility contribution to the stress supported by slip-links (expressed as $\sigma_s(\lambda, \alpha, \eta = 0.234)/\sigma_s(\lambda, \alpha = 0, \eta = 0.234) - 1$) is higher than that supported by crosslinks ($\sigma_c(\lambda, \alpha)/\sigma_c(\lambda, \alpha = 0) - 1$) and further increases with increasing η.

3.4. Combination of the James–Guth equation with the C_2 term

The above experiment–theory comparisons have shown that none of the three theoretical equations (JG, K, EV) can be utilised for the purpose outlined in Section 1. Therefore, further possibility has been sought in an extension of the Morris approach [22].

The power series approximation contained in the Morris equation limits its applicability to the low- and medium-elongation region. This a priori restriction can be removed by combining the C_2 term with the non-approximative result of the Langevin theory. For this purpose, the James–Guth Eq. (8) is used here. Its combination with the C_2 term gives a three-parameter equation, which in the following text will be denoted as the *JGC2 equation*:

$$\sigma = 2C_1(\lambda_m/3)\{\mathscr{L}^{-1}(\lambda/\lambda_m) - (1/\lambda^{3/2})\mathscr{L}^{-1}(1/\lambda^{1/2}\lambda_m) + 2C_2(1 - 1/\lambda^3) \quad (20)$$

In the low-elongation region and for not too small λ_m values, the JGC2 equation reduces to the two-parameter Mooney–Rivlin Eqs. (6) and (7) with the initial slope of 6 ($C_1 + C_2$). From the theory and previous studies, one expects C_1 to be proportional to the concentration of independent circuitous paths which is determined in the first place by stable network junctions, i.e. by chemical junction points and by some kind of stable (non-sliding) entanglements. The interpretation of the C_2-effect has been mentioned previously. In the high-elongation region, the stress is increasingly determined by λ_m, which in non-perfect networks may be related to the number Z_{ce} of segments between elastically effective junction points (chemical junctions and stable entanglements)

$$\lambda_m \approx Z_{ce}^{1/2} \quad (21)$$

$$Z_{ce} = M_{ce}/M_s$$

M_{ce} is the molar mass of elastically effective network chains which for tetrafunctional junctions may be approximated by the molar mass per twofold concentration of network junctions: $M_{ce} \approx \rho/2(C + E)$. C (mol/m^3) is the concentration of

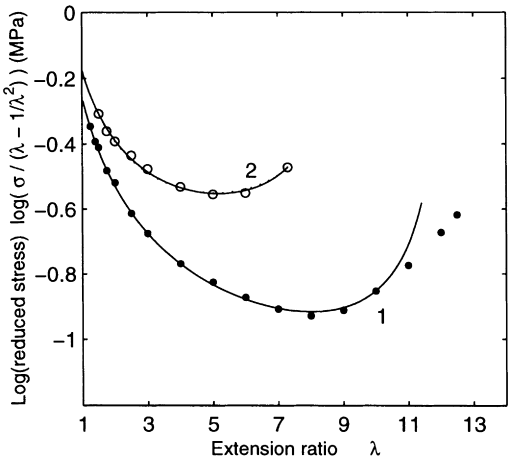

Fig. 8. Comparison of the Ikeda data [29,30] on two SBR networks (points) with the JGC2 equation (full curves) and with the JGMR equation (dashed curve) for parameter-values given in Table 2. 1—SBR A, 2—SBR C.

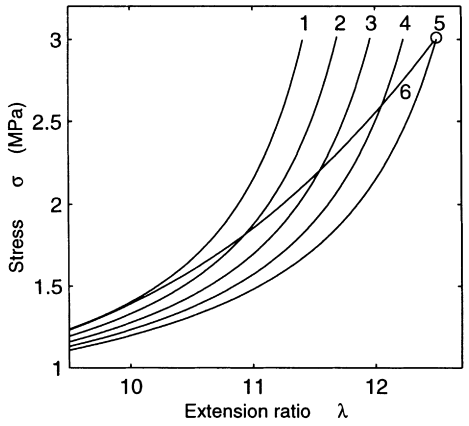

Fig. 9. Graphical determination of the dependence of λ_m on λ for SBR A network. Curves 1–5 are drawn using the JGC2 equation with $C_1 = 0.019_8$ MPa, $C_2 = 0.255$ MPa, and following λ_m-values: curve 1, 12.2; 2, 12.515; 3, 12.83; 4, 13.145; 5, 13.46. Curve 6 is experimental.

chemical junction points, E (mol/m^3) is the concentration of stable entanglements.

An alternative to the JGC2 equation is discussed briefly in Appendix A.

3.5. Experimental testing of the JGC2 equation

The first experimental test of the proposed Eq. (20) is shown in Fig. 8. The quasi-equilibrium data of Ikeda et al. [29,30] on two amorphous (i.e. non-strain-crystallising) networks of SBR (see Table 1) are plotted in co-ordinates of log(reduced stress) vs. extension ratio. The curves are drawn using Eq. (20) and the parameter values given in Table 2. The latter are chosen so as to obtain a good fit in the low-to-medium-elongation region and at least in the initial part of the high-elongation region. Description of the data up to break is satisfactory in the case of the more highly crosslinked network SBR C, the high-elongation region of which, however, is rather narrow. With the lightly crosslinked network SBR A, the high-elongation region is wide and the JGC2 curve is not able to describe it up to the break. Somewhere above the minimum of the reduced stress, the calculated stress begins to ascend at a higher rate than does the experimental stress. In other words, when approaching elongation at break, the experimental stress is increasingly lower than the theoretical stress predicted from the knowledge of the behaviour in the low-to-medium-elongation region and in the initial part of the high-elongation region.

The following interpretation of the observed phenomenon is offered. The negative deviation of the experimental stress from the calculated curve is a non-equilibrium effect. It is related to stress relaxation, which may be ascribed to some kind of stress-induced reorganisation of the network structure (topology). The latter begins to take place above the inflexion point and its extent increases with increasing elongation. As a result, the three parameters of Eq. (20) may be expected to be no longer constant. In the vicinity of the inflexion point, they will become functions of the extension ratio. The C_1 parameter and the C_2 parameter may be expected to decrease and the λ_m parameter to increase.

[Microscopically, this could mean that some independent circuitous paths are disappearing from the system while the average size of the circuitous paths increases. A possible mechanism can be imagined. Entanglements contributing to C_1—in spite of behaving as stable network junctions in the low-elongation region—may be forced by the increasing

Table 1
Crosslinking systems of SBR networks and conditions of measurements (SBR: emulsion radical copolymer of butadiene and styrene (23%); all four crosslinking systems contain ZnO and stearic acid in usual amounts)

Network	SBR A[a]	SBR B	SBR C[a]	SBR D[b]
Sulphur (phr[c])	0.5	0.5	1	2
Accelerator MOR[d] (phr[c])	0.5	0.5	1	–
Accelerator CBS[e] (phr[c])	–	–	–	0.8
Silane TESPT[f] (phr[c])	–	4	–	–
Test specimen	Ring	Dumbbell	Ring	Dumbbell
Strain rate (mm/min)	100	50	100	10

[a] SSD data of Ikeda et al. [29,30].
[b] SSD data of Klüppel and Heinrich [34].
[c] phr: mass parts per 100 mass parts of rubber.
[d] 2-(morpholinosulfanyl)benzothiazole.
[e] *N*-cyclohexylbenzothiazole-2-sulfenamide.
[f] bis[3–(triethoxysilyl)propyl] tetrasulfide.

Table 2
Parameter values of the JGC2 and JGMR equations for SBR networks

Parameters	SBR A[a]	SBR C[a]	SBR C[b]
C_1 (MPa)	0.019_8	0.073	0.065
C_2 (MPa)	0.255	0.260	0.265
λ_m	12.2	9.55	10.1

[a] The JGC2 equation (Eq. (20)).
[b] The JGMR equation (see Appendix A).

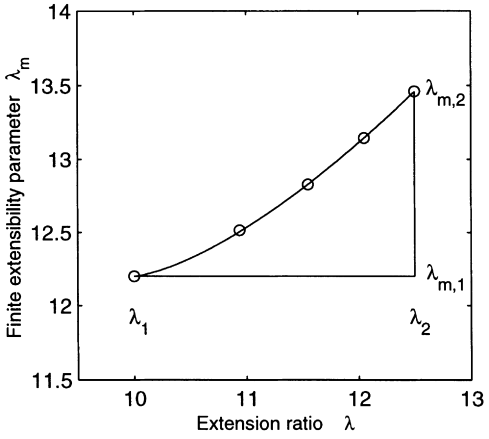

Fig. 10. Dependence of λ_m on λ determined for the SBR A network using a graphical method (Fig. 9). Curve is drawn using Eq. (22) and parameter values given in Table 3.

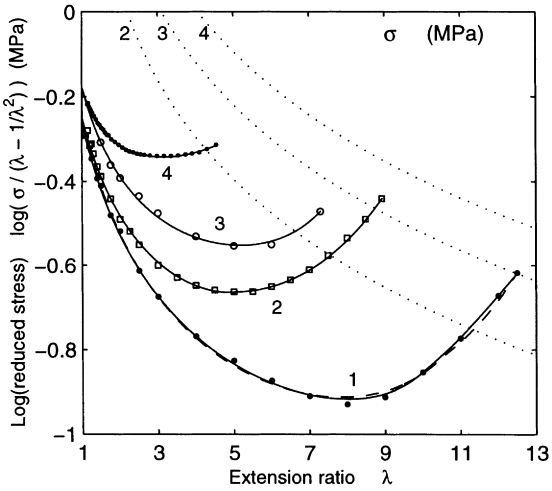

Fig. 11. Comparison of the SSDs of four SBR networks (points) with the JGC2L equation (full curves) and with the JGMRL equation (SBR A, dashed curve). Co-ordinates: log(reduced stress) vs. extension ratio. Dotted curves: curves of constant stress with stress values indicated. 1—SBR A. 2—SBR B. 3—SBR C. 4—SBR D. Networks composition and parameter values are given in Tables 1 and 3.

stress to accomplish movements along the network chains. This would change the network topology and lead to an increase in the network mesh size which would partially persist on retraction and recover slowly in the undeformed state. High-elongation hysteresis, time-dependent tension set and anisotropy can be envisaged as possible consequences. In very lightly crosslinked networks, permanent flow might be another factor contributing to the high-elongation stress relaxation, to the growth of λ_m and build-up of tension set.]

Information on the changes of parameter values with increasing extension ratio could possibly be obtained by studying the stress–elongation–retraction cycles as functions of the extension ratio amplitude. Instead of making such a study, a simplified data analysis is performed here. It is based on the fact that in the region of very high tensile strain, the stress is dominated by the value of the λ_m parameter. Therefore, it is assumed here that only the λ_m parameter is a function of the extension ratio while the parameters C_1 and C_2 may be treated in the first approximation

Table 3
Parameter values and other properties of SBR networks (first elongation up to break)

Parameters and properties	SBR A	SBR B	SBR C	SBR D	SBR A
Equation	JGC2L[a]	JGC2L[a]	JGC2[b]	JGC2L[a]	JGMRL[c]
C_1 (Mpa)	0.019_8	0.043_8	0.073	0.135_6	0.012_2
C_2 (Mpa)	0.255	0.238	0.260	0.187	0.269
λ_1	10.0	5.1	–	2.50	10.5
λ_2	12.5	8.95	7.3	4.51	12.5
$\lambda_{m,1}$	12.2	8.0	–	5.60	13.3
$\lambda_{m,2}$	13.46	10.0	9.75	6.79	13.95
a	1.45	1.20	–	1.10	1.20
Ultimate properties:					
λ_b	12.5	8.95	7.3	4.51	12.5
σ_b (MPa)	3.01	3.23	2.46	2.19	3.01
Other properties:					
C_2/C_1	12.9	5.4	3.6	1.38	22.0
$2\,(C_1 + C_2)$ (MPa)	0.550	0.564	0.666	0.645	0.562
M_c[d] $\approx (\lambda_{m,2})^2 M_s$ (kg/mol)	34.4	19.0	18.1	8.76	–
C[e] $\approx \rho/(2M_c)$ (mol/m^3)	13.7	24.7	26.0	53.7	–
R_b[f] $= \epsilon_b/\epsilon_{m,2}$	0.923	0.883	0.720	0.606	–

[a] Eqs. (20) and (22).
[b] Eq. (20); $\lambda_2 = \lambda_b$; $\lambda_m = \lambda_{m,2}$.
[c] See Appendix A.
[d] Estimate of the molar mass of chains between crosslinks; $M_s = 0.19$ kg/mol [34].
[e] Estimate of the concentration of chemical crosslinks; $\rho = 940$ kg/m^3.
[f] Ratio of strain at break, $\epsilon_b = \lambda_b - 1$, and the finite extensibility parameter, $\epsilon_{m,2} = \lambda_{m,2} - 1$.

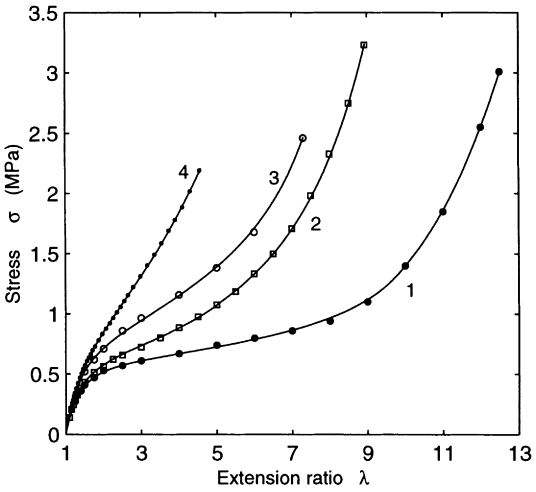

Fig. 12. Stress–strain dependences of Fig. 11 in linear co-ordinates. For legend, see Fig. 11.

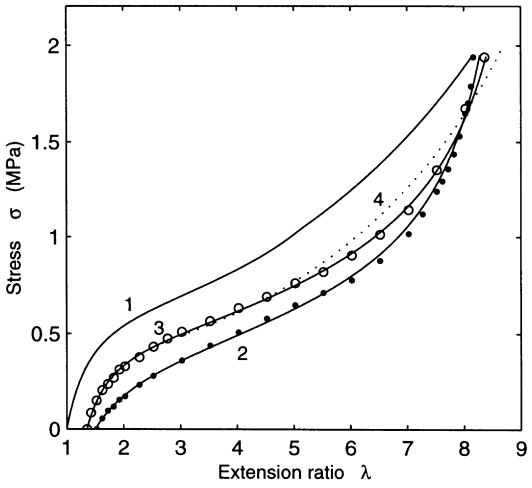

Fig. 13. Dependence of stress on extension ratio during repeated elongation of a SBR network. 1—first elongation, experimental points not shown, curve: JGC2L equation; 2—first retraction, full circles: experimental, curve: JGC2 equation; (3)—second elongation, open circles: experimental, full curve-JGC2 equation; (4)—second elongation, dotted curve calculated according to the Edwards–Vilgis equation. Parameter values for the curves are given in Table 4.

as independent of λ. With this assumption, the dependence of λ_m on λ may be obtained from comparison of experimental data with Eq. (20) using numerical methods, or, with the help of a simple graphical method which will be demonstrated now.

Curve 6 in Fig. 9 is the experimental SSD of the lightly crosslinked SBR A network plotted in linear co-ordinates. Curve 1 is drawn according to the JGC2 equation using the same parameter values as those used in Fig. 8 which were chosen to obtain a good fit in the low-to-medium elongation region and in the initial part of the high-elongation region. Curves 2–5 are drawn with gradually increasing values of λ_m. From the points of intersection of curve 6 with curves 2–5 one obtains the required dependence of λ_m on λ. It has been plotted in Fig. 10. As can be seen, up to $\lambda = \lambda_1 = 10$ the λ_m parameter is constant and equal to $\lambda_{m,1} = 12.2$. In the λ range from $\lambda_1 = 10$ to $\lambda_2 = 12.5$, λ_m increases from $\lambda_{m,1} = 12.2$ to $\lambda_{m,2} = 13.45$. This corresponds to an increase in Z_{ce} from 150 to 180, i.e. to an increase in the effective network mesh size of ca. 20%. This does not seem unreasonable. It should be noted that the stress-induced growth of λ_m is a reflection of a hysteretic mechanism, which is highly favourable from the point of view of ultimate properties, the increase in network extensibility being accompanied by an increase in tensile strength.

The dependence of λ_m on λ shown in Fig. 10 can be described by a simple power function

$$\lambda \le \lambda_1 : \lambda_m = \lambda_{m,1}$$

$$\lambda > \lambda_1 : \lambda_m = \lambda_{m,1} + (\lambda_{m,2} - \lambda_{m,1})\{(\lambda - \lambda_1)/(\lambda_2 - \lambda_1)\}^a \quad (22)$$

The meaning of λ_1, λ_2, $\lambda_{m,1}$, $\lambda_{m,2}$, a, follows from Fig. 10 and Eq. (22).

3.6. The JGC2L equation

In the following text, the combination of the JGC2 Eq. (20) with Eq. (22) will be denoted as the *JGC2L equation*. It contains seven parameters and for a given SBR network it offers a satisfactory description of the stress–strain dependence up to the break. (An alternative to the JGC2L equation, the JGMRL equation, is discussed briefly in Appendix A). It should be noted that only five of the seven parameters are adjustable. The quantity λ_2 is either chosen as the highest extension ratio in the experiment or is equal to the extension ratio at break. The quantity $\lambda_{m,2}$, the finite extensibility parameter at λ_2, is essentially determined by the values of the remaining parameters and has virtually no freedom of adjustment.

As can be seen in Fig. 11, the deviations of the experimental points from the JGC2L curve do not exceed some 3–4%. Since the sample was extended up to the break, the λ_2 parameter is equal to the extension ratio at break, λ_b. Its insertion for λ into the JGC2L equation gives the tensile strength, σ_b. Thus, the seven parameter values supply a full information on the stress–strain curve including its final point. A comparison of the JGC2L equation with experimental SSDs is shown in linear co-ordinates in Fig. 12, the parameter values being given in Table 3. The results on our own network, SBR B, and on the Klüppel–Heinrich network SBR D (see Table 1), are included in Figs. 11 and 12. For the SBR A, SBR B networks the C_2/C_1-ratio is very high (much higher than could be explained by the constrained-junction theory [18,19]). An increase in sulphur concentration and addition of tetrasulfide TESPT into the crosslinking system both lead to an increase in the crosslink concentration and to a decrease in the network mesh size. In

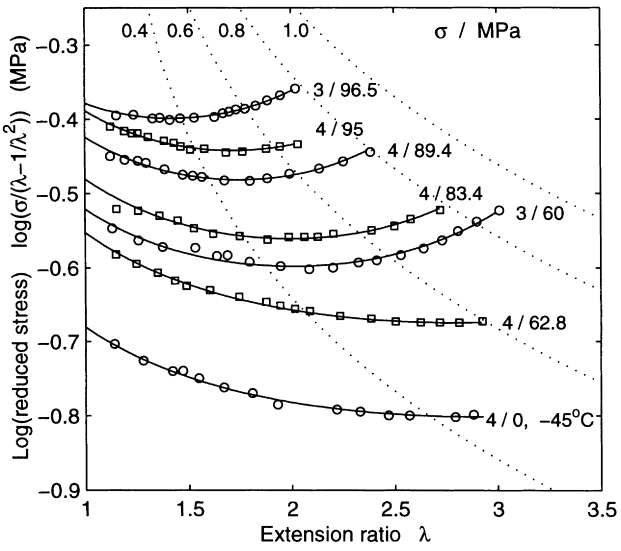

Fig. 14. Comparison of the SSDs of bimodal 1100/18 500 polysiloxane networks (points) with the JGC2 equation (curves). Parameter values are given in Tables 5 and 6. Functionality of the crosslinker and molar percentage of short chains are indicated on the curves. Dotted curves: curves of constant stress.

line with this is the increase in the C_1 parameter and the observed decrease in the limiting extensibility parameter $\lambda_{m,2}$. The latter effects are reflected by significant changes of the reduced stress in the medium and high-elongation region. On the other hand, at very low elongations, the effect of chemical crosslinking is obviously overshadowed by physical effects (entanglements of all kinds) and the initial reduced stress can be seen to be rather insensitive to chemical crosslinking, as also is the C_2 parameter.

An estimate of the network mesh size is calculated in Table 3 using the following simplifying arguments. While the limiting extensibility parameter $\lambda_{m,1}$ may perhaps still depend both on chemical crosslinks and on some entanglements ($\lambda^2_{m,2} \approx Z_{c,e}$), the $\lambda_{m,2}$ parameter is probably determined by the strongest network junctions only, i.e. by chemical junction points ($\lambda^2_{m,2} \approx Z_c$). Using the value of molar mass of statistical segment M_s quoted in the literature, one gets estimates of the molar mass of network chains M_c and, from these, estimates of the concentration C of chemical junctions. Values obtained seem quite reasonable. A sulphur dosage of 2 phr with 0.8 phr of sulfenamide accelerator leads to C around 50 mol/m^3 which is the usual value for such networks. Also, C of networks SBR A, C, D increases with sulphur dosage. The ratio, R_b, of the strain at break ϵ_b and the limiting extensibility parameter $\epsilon_{m,2} = (\lambda_{m,2} - 1)$ is a measure of effectivity with which the network is able to utilise the potential of its network mesh size. R_b is higher (92%) in the lightly crosslinked network SBR A with its more pronounced high elongation relaxation than in the highly crosslinked network SBR D (60%). In addition, the higher strain-rate of SBR A may have had some effect, too.

Elongation–retraction cycles. Two elongation–retraction cycles with the same stress amplitude were performed with the SBR B network. A comparison of these data with the JGC2L equation is complicated by the quasi-permanent change of the specimen length, i.e. by the time-dependent tension set. At the end of the first retraction, the length of the specimen was L_{s1}, the remaining extension ratio was $\lambda_{s1} = L_{s1}/L_o = 1.50$ and the apparent tension set was $TS_1 = (L_{s1} - L_o)/L_o = 0.5 = 50\%$ (see Table 4). The length of the specimen at rest decreased slowly with time and at the beginning of the second cycle it had a value of L_{s2}, the remaining extension ratio was $\lambda_{s2} = L_{s2}/L_o = 1.353$ and

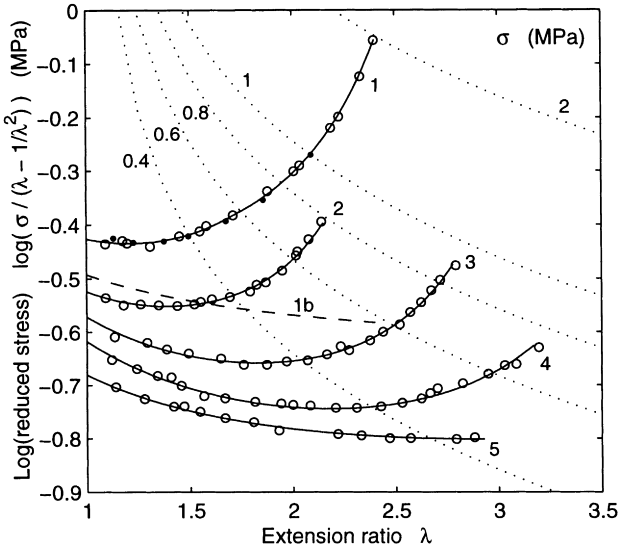

Fig. 15. Comparison of the SSDs of bimodal 220/18 500 polysiloxane networks (points) with the JGC2L equation (curve 1) and with the JGC2 equation (curves 2–5). Parameter values are given in Tables 6 and 7. Percentage of short chains ($M = 220$ g/mol) : 1, 90; 2, 90; 3, 75; 4, 60; 5, 0. Temperature of measurement: 1, + 25°C; 2–5, −45°C. Curve 1b is drawn according to the Mooney–Rivlin equation using the same C_1,C_2-values as in curve 1.

Table 4
Parameter values of the JGC2L and JGC2 equations for the SBR B network on repeated elongation (parameter values of the Edwards–Vilgis equation for 2nd elongation: $N_c kT = 0.12$ MPa, $N_s kT = 0.30$ MPa, $\eta = 0.234$, $\alpha = 1/16$)

Parameter	First elongation[a]	First retraction[b]	Second elongation[b]
C_1 (MPa)	0.042	0.042	0.042_5
C_2 (MPa)	0.220	0.080	0.143
λ_1	5.1	–	–
λ_2	8.1[c]	8.24	8.39_3[c]
$\lambda_{m,1}$	8.0	–	–
$\lambda_{m,2}$	10.0	9.0	9.62
a	1.20	–	–
Tensile set		0.50[d]	0.353[e]

[a] Parameters of the JGC2L equation.
[b] Parameters of the JGC2 equation, $\lambda_m = \lambda_{m,2}$.
[c] Amplitude of the extension ratio on elongation.
[d] Immediately after the end of retraction.
[e] 5 min after the end of retraction, at the beginning of the 2nd elongation.

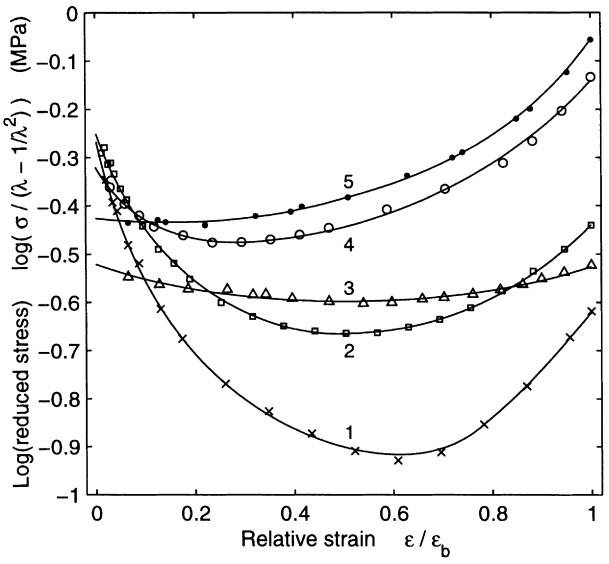

Fig. 16. Comparison of the experimental SSDs (points) with the JGC2L equation (full curves). Co-ordinates: log(reduced stress) vs. relative strain (ratio of strain and strain at break). Parameter values are given in Tables 3, 5 and 7. 1—SBR A; 2—SBR B; 3—poly(dimethylsiloxane), *M*: 1100 60%, 18 500 40%, $f = 3$; 4—NR 100°C; 5—poly(dimethylsiloxane), *M*: 220 90%, 18 500 10%, $f = 4$, 25°C.

$TS_2 = 0.353$. To compare the first retraction and second elongation–retraction data with the JGC2L equation, a corrected extension ratio is defined as the difference between the nominal extension ratio and tension set: $\lambda_{cor} = \lambda - TS = (L - L_s)/L_o$ (dropping the numbers 1, 2, in the subscript). Curves 2 and 3 in Fig. 13, which were obtained from the comparison of the JGC2L equation with experimental data based on corrected extension ratios, are then shifted to the right by TS_1 and TS_2, respectively, to be comparable with the nominal (uncorrected) λ values of the experiment.

On first elongation, the SSD is satisfactorily described by the JGC2L equation, with the λ_m parameter increasing from 8 to 10. The retraction curve can be roughly described by the JGC2 equation and the approximate constancy of λ_m seems to indicate that on retraction, the network structure (the network mesh size) is remaining essentially in the state attained at the end of the first elongation. The second-elongation data can be described by the JGC2 equation quite well. In spite of having introduced some semipermanent change of length and thus a certain anisotropy into the unstressed specimen, prestraining seems to have simplified the network structure, at least temporarily. This leads to a behaviour which—but for a small C_2 contribution—approaches that predicted by the Langevin theory. Such a result conforms to the proposed molecular picture.

The data in Fig. 13 are also compared with the Edwards–Vilgis equation (dotted curve). A satisfactory data description cannot be achieved not even when the slip parameter is varied. The slope of the calculated curve in the high-elongation region remains smaller than that of the experiment. This feature is obviously due to the approximation introduced into the theoretical treatment [5] by using the simple probability distribution (4.19) in place of a more exact one (Langevin) to model the singularity of entropy.

Bimodal poly(dimethylsiloxane) networks. Poly(dimethylsiloxane) networks containing very short and relatively long network chains were prepared by Mark and co-workers [35–38] who studied their stress–strain behaviour under conditions approaching elastic equilibrium. Unlike conventional poly(dimethylsiloxane) networks, these bimodal end-linked networks show pronounced effects of limited chain extensibility, i.e. an upturn of reduced stress. Evidence was obtained that strain-induced crystallisation is not taking place. The stress–strain behaviour of bimodal networks was approached theoretically in several papers (cf. Ref. [2, chap. 13]) and a qualitative description was obtained.

Some of the data obtained on networks based on chains with $M = 1100$ and 18 500 g/mol are compared with the three-parameter JGC2 equation in Fig. 14. The resulting parameter values are given in Table 5. The degree of fit to the data is very good. Another example is shown in Fig. 15 and Table 6 for 220/18 500 networks [38] measured at −45°C (curves 2–5). A network containing 90 mol% of short chains ($M = 220$ g/mol) and measured at + 25°C [37] has a relatively wide high-elongation region and a much higher (double) tensile strength than any of the other bimodal networks (curve 1). To describe its SSD the JGC2L equation had to be used (parameter values are given in Table 7).

Table 5
Parameter values of the JGC2 equation and other properties of bimodal poly(dimethylsiloxane) networks. Data of Andrady et al. [35,36], equilibrium measurements, 25°C

c[a]	60	62.8	83.4	89.4	95.0	96.5
f[b]	3	4	4	4	4	3
M_n (kg/mol)[c]	8.06	7.57	3.99	2.94	1.97	1.71
C_1 (MPa)	0.077	0.072	0.081	0.096	0.105_5	0.130
C_2 (MPa)	0.068	0.066	0.078	0.082	0.087_3	0.061_5
λ_2[d] ($\approx \lambda_b$)	3.01	2.93	2.73	2.38	2.03	2.02
λ_m	4.20	6.50	4.06	3.54	3.49	3.19
C_2/C_1	0.88	0.92	0.96	0.85	0.83	0.47
$2(C_1 + C_2)$ (MPa)	0.290	0.276	0.318	0.356	0.386	0.383
M_s (kg/mol)[e]	0.46	0.18	0.24	0.24	0.16	0.17
R_b[f] $= \epsilon_b/\epsilon_m$	0.63	0.35	0.56	0.54	0.41	0.46

[a] Molar percentage of short (hydroxy-terminated) polysiloxane chains ($M = 1100$ g/mol) in their mixture with long chains ($M = 18\,500$ g/mol).
[b] Functionality of the crosslinker (vinyltriethoxysilane, tetraethoxysilane).
[c] Number-average molar mass of the mixture of polysiloxane chains prior to crosslinking.
[d] The highest extension ratio attained in the measurement, generally equal to the extension ratio at break, λ_b.
[e] Estimate of the molar mass of the statistical segment, M_n/λ_m^2.
[f] Ratio of strain at break, $\epsilon_b = \lambda_b - 1$, and the limiting extensibility parameter, $\epsilon_m = \lambda_m - 1$.

Table 6
Parameter values of the JGC2 equation and other properties of bimodal poly(dimethylsiloxane) networks. Data of Zhang and Mark [38], equilibrium measurements, −45°C (for explanation of other symbols see Table 5)

c[a]	0	60	75	90
C_1 (MPa)	0.055_5	0.049_2	0.052_3	0.072_7
C_2 (MPa)	0.047_5	0.082	0.075	0.061
$\lambda_2(\approx \lambda_b)$	2.9	3.18	2.79	2.16
λ_m	(7.0)	3.93	3.27	2.63
C_2/C_1	0.86	1.67	1.43	0.84
$2(C_1 + C_2)$ (MPa)	0.206	0.262_4	0.254_6	0.267_4
M_n (kg/mol)	18.5	7.53	4.79	2.048
M_s (kg/mol)	(0.38)	0.48	0.45	0.30
$R_b = \epsilon_b/\epsilon_m$	0.32	0.74	0.79	0.71

[a] Molar percentage of short (hydroxy-terminated) polysiloxane chains (M = 220 g/mol) in their mixture with long chains (M = 18 500 g/mol); crosslinker: tetraethoxysilane.

The average molar mass of network chains M_c of bimodal networks may be taken approximately equal to the number-average molar mass, M_n, of chains used to prepare these networks if a simple idealised course of the end-linking reaction is assumed. Combining this information with the experimentally obtained limiting extensibility parameter λ_m, we arrive at an estimate of the molar mass of statistical segment: $M_s = M_c/\lambda_m^2$. The values obtained are given in Tables 5–7. They are scattered over a rather wide range, seem to be somewhat lower for 1100/18 500 networks (around 0.2 kg/mol, with one exception) than for the 220/18 500 networks (0.30–0.48 kg/mol) but do not show any apparent trend with the percentage of short chains in admixture with long chains. Curve 1b in Fig. 15 is drawn according to the Mooney–Rivlin equation using the C_1 and C_2 values obtained in curve 1 for the JGC2L equation. The difference between the curves 1 and 1b is thus equal to the finite-extensibility contribution to the stress. In the limit of $\lambda \rightarrow 1$, it amounts to ca. 15%. Processing of data on the basis of the JGC2, JGC2L equations leads to somewhat lower values of C_1 and higher values of C_2 than are those resulting from direct comparison of data with the Mooney–Rivlin equation [35–38]. As a result, conclusions reached here differ in some respect from those of Mark et al. With few exceptions, the C_2 values are virtually constant and the values of $2(C_1 + C_2)$ differ significantly from those of $2C_1$. According to the affine theory and assuming a perfect network structure ($M_c = M_n$, zero sol fraction), the modulus of bimodal tetrafunctional networks should be given by the relation $2(C_1 + C_2) = A\rho RT/M_n$, with $A = 1$. Calculation of the A parameter from the data in Table 6 gives values of ca. 2, 1, 0.7 and 0.3. This result suggests that the structure of the networks in question may differ from the idealised picture.

The R_b values of bimodal networks range from 0.3 to 0.8 and R_b of the best bimodal network (Table 7) approaches that of the NR network measured at 100°C.

Table 7
Parameter values of the JGC2L equation and other properties of a bimodal poly(dimethylsiloxane) network (PDMS) and a NR network (poly(dimethylsiloxane) network: 90 mol% M = 220 g/mol, 10 mol% M = 18 500 g/mol, tetraethoxysilane; equilibrium measurements at 25°C, data [37], $M_c \approx M_n$. NR network: sulphur/accelerator vulcanised natural rubber; equilibrium SSD measured at 100°C, data [39]. Concentration of chemical crosslinks C for a NR network crosslinked with 2 phr of sulphur and 1 phr of thiazole accelerator is assumed to have the usual value around 50 mol/m^3; from this, $M_c = \rho/2C$ = 9.2 kg/mol.)

Parameters and properties	PDMS	NR
C_1 (MPa)	0.109	0.117
C_2 (MPa)	0.052	0.120
λ_1	1.70	4.0
λ_2	2.39	9.5
$\lambda_{m,1}$	2.52	8.2
$\lambda_{m,2}$	2.67	10.9
a	1.10	1.10
C_2/C_1	0.48	1.03
$2(C_1 + C_2)$ (MPa)	0.322	0.474
λ_b	2.39	9.5
σ_b (MPa)	1.96	7.0
M_c (kg/mol)	2.048	9.2
$M_s \approx M_c/\lambda_{m,2}^2$ (kg/mol)	0.29	0.077
$R_b = \epsilon_b/(\lambda_{m,2} - 1)$	0.832	0.859

Comparison of networks based on different polymers. Fig. 16 compares the SSDs of two SBR networks, two bimodal poly(dimethylsiloxane) networks and a natural rubber network [39] measured at 100°C (parameter values in Table 7). The stress-induced crystallisation of the NR network probably does not vanish completely at 100°C but may be expected to be largely suppressed. Its contribution to birefringence becomes almost insignificant [39]. In Fig. 16, the logarithm of reduced stress is plotted vs. the relative strain (i.e. tensile strain divided by strain at break). It is interesting to note that a major part of the relative SSD of the high-strength bimodal poly(dimethylsiloxane) network (curve 5) is very similar to that of the NR network measured at 100°C (curve 4) although the two networks differ in their strain at break enormously. In the region of relative strain from 0.2 to 1, the two networks differ only by a constant, the reduced stress of the NR network being lower by ca. 12%. At relative strains decreasing below 0.2, the reduced stress of the NR network increases more rapidly and, in the limit of zero strain, becomes higher than that of the poly(dimethylsiloxane) network. This is reflected in the higher C_2 value of the NR network and may be ascribed to a higher entanglement concentration in polyisoprene than in poly(-dimethylsiloxane). The reduced stresses at break of both networks are higher than the respective initial ones. In SBR, the low-elongation contribution of entanglements to the stress is obviously very high. The curves of lightly crosslinked SBR show a very deep minimum and the reduced stress at break is lower than the initial one for all four SBR networks. The course of the curves in Fig. 16 suggests that with increasing relative strain, the effect of physical interactions (e.g. entanglements of all kinds) progressively

diminishes and that the high-elongation behaviour is dominated by strong network junctions, i.e. by crosslinks of chemical type.

An estimate of $M_s = 0.077$ kg/mol (i.e. 1.13 monomer units per statistical segment) has been obtained for the NR network using a plausible assumption regarding its chemical crosslink concentration (Table 7). The result obtained is much lower than that found by Morris [1,22] (4.3 monomer units per segment) and approaches the value derived theoretically on the basis of a freely rotating chain model (0.77 monomer units per segment [1]).

4. Conclusions

1. The tensile stress–strain dependences predicted by the eight-chain model of Arruda and Boyce are virtually the same as those predicted by the three-chain model of James and Guth if comparison is made at the same value of the finite extensibility parameter λ_m and at (nearly) equal value of the modulus G.
2. The three-parameter van der Waals equation does not give a satisfactory description of stress–strain dependences of lightly crosslinked SBR networks.
3. The four-parameter slip-link-model equation does not give a satisfactory description of experimental stress–strain dependences if the slip-parameter is prescribed its theoretical value. If all four parameters are allowed to be adjusted, then the data description becomes possible in some cases but the parameters may assume unrealistic values. The theoretical prediction according to which the limiting extensibility is determined by the entanglement distance and does not depend on chemical crosslink concentration is not supported by experiment.
4. The proposed three-parameter combination of the James–Guth equation with the C_2 term of the Mooney–Rivlin equation—the JGC2 equation—offers a satisfactory description of stress–strain data obtained on pre-strained amorphous SBR networks and on a number of bimodal polysiloxane networks.
5. The stress–strain dependences up to break of unprestrained amorphous SBR networks, of some bimodal polysiloxane networks and of a NR network with a suppressed strain-induced crystallisation can be described by the seven-parameter JGC2L equation which is the JGC2 equation with a strain-dependent finite-extensibility parameter λ_m. The dependence of λ_m on extension ratio λ is obtained from comparison of experimental data with the JGC2 equation and can be described by a simple power function. The experimental stress–strain dependences are described by the JGC2L equation with an accuracy better than 3–4% and the information given by the values of the seven parameters (only five of them being adjustable parameters) includes the ultimate properties. Thus, the JGC2L equation may be utilised for purpose of data storage while yielding information on network structure and predicting behaviour on repeated elongation.
6. The observed increase in the finite-extensibility parameter with strain is ascribed to a stress-induced reorganisation (simplification) of the network structure that persists on retraction and on subsequent extension. Stress-induced increase in network mesh size is proposed as a possible factor, with semipermanent flow contributing in very lightly crosslinked networks.
7. The applicability of the JGC2L equation to filler- and hard domain-reinforced networks will be shown in the next paper.

Acknowledgements

The author is greatly indebted to the Grant Agency of the Czech Republic for financial support of this work within the grant project No. 203/98/0884.

Appendix A

The James–Guth equation may in principle be combined with the Mooney–Rivlin equation in the following way as well:

$$\sigma = (2C_1 + 2C_2/\lambda)(\lambda_m/3) \times \{\mathscr{L}^{-1}(\lambda/\lambda_m) - 1/\lambda^{3/2})\mathscr{L}^{-1}(1/\lambda^{1/2}\lambda_m)\}$$

This equation, which we denote as the *JGMR equation*, implies that the limiting extensibility affects both the C_1 and the C_2 terms. In this respect, it is analogous to the Edwards–Vilgis equation where both the crosslinks term and the sliding entanglements term include functions of the limiting extensibility parameter. In the JGC2 equation, the C_2-term contribution to the stress attains a practically constant value at extension ratios higher than ca. 3 and no further rise of this term is expected at high elongations. According to the JGMR equation, the C_2-term contribution to the stress at first increases, levels off to a constant value at medium elongations and begins to increase again at high elongations. In our opinion the latter behaviour is less probable.

In Fig. 8 the JGMR equation is seen to describe the SSD of the SBR C network satisfactorily. The C_1 value is slightly lower and the C_2 and λ_m values are slightly higher than are those obtained for the JGC2 equation (Table 2).

The *JGMRL equation* is an analogy of the JGC2L equation. It implies that in the JGMR equation the limiting extensibility parameter λ_m may change with λ. The JGMRL equation is compared with an experimental SSD in Fig. 11 and the degree of fit to the data is slightly worse than that

obtained with the JGC2L equation. Also, the C_1 value (Table 3) seems to be too low.

References

[1] Treloar LRG. The physics of rubber elasticity. 3rd ed. Oxford: Clarendon Press, 1975.
[2] Erman B, Mark JE. Structure and properties of rubberlike networks. New York: Oxford University Press, 1997.
[3] James HM, Guth E. J Chem Phys 1943;11:455.
[4] Kilian HG. Polymer 1981;22:209.
[5] Edwards SF, Vilgis TA. Polymer 1986;27:483.
[6] Kuhn W. Kolloid Z 1936;76:258.
[7] James HM, Guth E. Ind Engng Chem 1941;33:624.
[8] James HM, Guth E. J Chem Phys 1953;21:1039.
[9] Wall FT. J Chem Phys 1942;10:132.
[10] Wall FT, Flory PJ. J Chem Phys 1951;19:1435.
[11] Flory PJ. Macromolecules 1982;15:99.
[12] Mooney M. J Appl Phys 1940;11:582.
[13] Rivlin RS. Philos Trans R Soc 1948;A241:379.
[14] Mullins L. J Appl Polym Sci 1956;19:225.
[15] Moore CG, Watson WF. J Appl Polym Sci 1956;19:237.
[16] Meissner B. J Polym Sci 1967;C16:781.
[17] Meissner B, Klier I, Kuchařík S. J Polym Sci 1967;C16:793.
[18] Flory PJ, Erman B. Macromolecules 1982;15:800.
[19] Erman B, Flory PJ. Macromolecules 1982;15:806.
[20] Ball RC, Doi M, Edwards SF, Warner M. Polymer 1981;22:1010.
[21] Arruda EM, Boyce MC. Mech Phys Solids 1993;41:389.
[22] Morris MC. J Appl Polym Sci 1964;8:545.
[23] Klüppel M. Macromolecules 1994;27:3596.
[24] Klüppel M. Macromolecules 1994;27:7179.
[25] Kilian HG, Strauss M, Hamm W. Rubber Chem Technol 1994;67:1.
[26] Vilgis TA. Prog Colloid Polym Sci 1987;75:4.
[27] Vilgis TA. Kautsch Gummi Kunstst 1989;42:475.
[28] Kilian HG, Vilgis TA. Colloid Polym Sci 1984;262:15.
[29] Ikeda Y, Tanaka A, Kohjiya S. J Mater Chem 1997;7:455.
[30] Ikeda Y, Tanaka A, Kohjiya S. J Mater Chem 1997;7:1497.
[31] Thirion P, Weil T. Polymer 1984;25:609.
[32] Brereton MG, Klein PG. Polymer 1988;29:970.
[33] Mullins L. J Appl Polym Sci 1959;2:257.
[34] Klüppel M, Heinrich G. Macromolecules 1994;27:3596.
[35] Andrady AL, Llorente MA, Mark JE. J Chem Phys 1980;72:2282.
[36] Andrady AL, Llorente MA, Mark JE. J Chem Phys 1980;73:1439.
[37] Llorente MA, Andrady AL, Mark JE. J Polym Sci, Polym Phys Ed 1981;19:621.
[38] Zhang Z-M, Mark JE. J Polym Sci, Polym Phys Ed 1982;20:473.
[39] Treloar LRG. Trans Faraday Soc 1947;43:284.